Experimental Evaluation of Kaiser Bolted Bracket Steel Moment-Resisting Connections

SCOTT M. ADAN and WILLIAM GIBB

The Kaiser bolted bracket (KBB) is a new beam-to-column moment connection that consists of proprietary cast high-strength steel brackets that are fastened to the flanges of a beam and then bolted to a column. This fully restrained connection is designed to eliminate field welding in steel moment frame construction.

The cast Kaiser brackets are manufactured in a variety of sizes and are proportioned to develop the probable maximum moment capacity of the connecting beam. Depending on fabrication preference the brackets can be either fillet welded [Figure 1(a) or bolted to the beam Figure 1(b)]. When subjected to cyclic inelastic loading, yielding and plastic hinge formation occur primarily in the beam near the end of the bracket, thereby eliminating inelastic deformation demands at the face of the column.

This paper summarizes the development of bolted bracket connections and presents the results of seven full-scale KBB tests. These tests were conducted to evaluate the connection for both the retrofit of existing and the construction of new steel moment frames. More specifically, the tests were intended to assess the ductility of the connection under cyclic inelastic loading and to qualify their performance with respect to the requirements of ANSI/AISC 341, *Seismic Provisions for Structural Steel Buildings* (AISC, 2005a), hereafter referred to as the AISC *Seismic Provisions*.

BACKGROUND

In the aftermath of the 1994 Northridge, California, earthquake, damage to steel moment frame connections spawned concern for the reliability of established design and construction procedures. Widespread damage was observed in beam-to-column joints that experienced rotation levels well below the plastic moment capacity of the framing members. Failures included nonductile fractures of the bottom girder flange-to-column flange complete-joint-penetration (CJP) groove welds, cracks in beam flanges and cracks through the column section (Tremblay et al., 1995; Youssef et al., 1995; FEMA, 2000). The fractures were caused by poor welding procedures, including the use of filler metals with inherent low toughness, uncontrolled deposition rates and inadequate quality control; connection design and detailing that led to larger moment-frame members, less system redundancy and higher strain demands on the connections; the use of higher strength girders, leading to unintentional undermatching of the welds; and a number of other connection detailing and construction practices that were typical prior to the earthquake (FEMA, 2000). In an attempt to ensure satisfactory earthquake performance, more stringent qualifications for fully restrained moment connections were imposed.

Subsequent to the earthquake, a significant amount of research activity was initiated on the behavior of fully restrained connections. Some of the research objectives were focused specifically on providing a bolted repair method for moment frame connections damaged during the earthquake. Implementation of a bolted repair has advantages that come from eliminating the health and fire hazards associated with welding in an occupied building. Eliminating field welding can also reduce costs associated with weld fabrication and inspection.

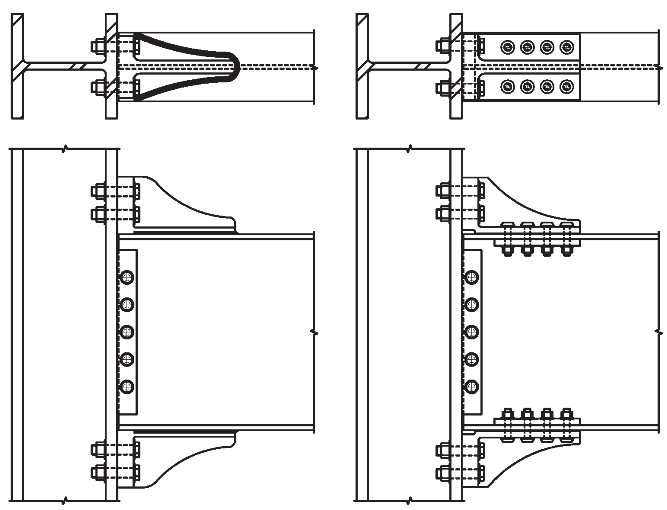

(a) Fillet welded to the beam. *(b) Bolted to the beam*

Fig. 1. Typical Kaiser bolted bracket moment-resisting connection.

Scott M. Adan is a structural engineer at Simpson Gumpertz & Heger Inc., San Francisco, CA.

William Gibb is the president of Steel Cast Connections, LLC, Seattle, WA.

A research program was initiated at Lehigh University with the objective of developing an economically viable bolted connection repair that could restore damaged moment connections to their original fully rigid condition. The program developed two repair schemes using high-strength bolts to attach a bracket between the flanges of a beam and a column. In the first scheme, the brackets were fabricated from either a stiffened angle or from thick welded plates. In the second scheme, the bracket consisted of pipes welded to a horizontal bracket plate.

The effectiveness of the repair schemes were demonstrated experimentally at Lehigh University where a total of eight tests were performed (Kasai et al., 1998). The first four specimens utilized relatively lightweight wide flange beam (W16×40) and column (W12×65) sections, identical to specimens tested by Anderson and Linderman (1991) with a clear span-to-depth ratio of 15. The haunch brackets were fabricated from a trimmed W14×145 section and fitted with a welded vertical stiffener plate. The beams, columns and brackets were A572 Grade 50 steel. The connecting fasteners were high-strength pretensioned A490 bolts.

The subsequent four test specimens utilized heavier wide flange beam (W36×150) and column (W14×426) sections, identical to specimens tested by Engelhardt and Sabol (1994) with a clear span-to-depth ratio of 10. The columns were A572 Grade 50 and the beams were A36 steel. The haunch brackets were fabricated from thick welded steel plates and connected with A490 bolts.

On five of the specimens, brackets were connected to both top and bottom beam flanges. The other three specimens being configured with brackets bolted only to the bottom flange, the top flange being connected with a high notch toughness CJP weld. This revised configuration was intended to investigate the effects of repairing only a fractured bottom flange. When a beam flange was connected with a bracket, the associated flange was not welded to the column, simulating a fractured condition.

On six of the specimens, thick steel washers or clamp plates were positioned on the opposite side of the connected beam flange in order to prevent ductile fracture through the net area. The clamp plates maintain the stability of the flange when inelastic buckling occurs outside the connected region.

Additionally, on three of the specimens, a thin brass washer plate was inserted between the bracket and the beam flange. In previous research, Grigorian et al. (1993) had used a thin brass plate as a friction-based seismic energy dissipator. Although not intended to dissipate energy in the bolted bracket connection, the brass plate provides a smooth slip mechanism at the bracket-to-beam interface.

All eight tested specimens exceeded the AISC *Seismic Provisions* (AISC, 2005a) special moment frame (SMF) qualifying requirements. At higher levels of interstory drift, flange local buckling outside the bracket region was observed to increase strains in the outermost bracket bolt holes. In the lighter specimens without the clamp plates, this increased strain caused necking and fracture through the flange net area. When configured with the clamp plates, the identical specimens exceeded the required interstory drift requirement without failure, and the tests were subsequently halted to prevent damage to the apparatus.

In the heavier specimens configured without the thin brass washer plates, energy released through the beam-bracket slip-stick mechanism caused loud, intermittent bursts of noise, particularly at high levels of inelastic drift. Fracture occurred through the flange net area at the outermost bolt holes. Upon inspection, evidence of abrading was observed between the beam and bracket contact surfaces. When the identical specimen was configured with the thin brass washer plates, deformation and fracture occurred outside the connected region through the flange gross area at a higher level of interstory drift. Noise levels were reduced and no evidence of abrading was observed.

Based on the initial eight Lehigh tests, the research concluded that the bolted bracket was capable of restoring the capacity of weakened or damaged moment connections. The haunch brackets directed yielding and inelastic beam deformation away from the column face and outside the connected region.

Although testing demonstrated that the thin brass washer and clamp plates were not essential in achieving the qualifying level of interstory drift, the research concluded that the plates could enhance ductile behavior and prevent net area fracture. The thin brass washer plate in particular was attributed with providing a smooth slip mechanism between the bracket and beam flange (Kasai et al., 1998).

To further demonstrate the effectiveness of the bolted bracket connection repair, six additional tests were performed at Lehigh University (Gross et al., 1999). The additional tests sought to obtain data on interior or two-sided connections that included the presence of a concrete slab.

In order to investigate the effects of repairing only a fractured bottom flange, the specimens were configured with brackets fastened only to the beam bottom flange. However, unlike prior tests, the top flange was fastened with a pre-Northridge CJP weld using filler metals without rated notch toughness and the backer bar was left in place. The bottom flange haunch brackets were fabricated from welded plates and attached with both a thin brass washer plate at the bracket slip interface and clamp plates opposite the connected bracket. The clear span-to-depth ratio of the specimens varied between 8 and 10. The beam, column and brackets were all A572 Grade 50 steel.

The first four specimens showed poor inelastic drift performance developing early fractures in the top flange CJP weld. In order to enhance the performance of the remaining two specimens, a double angle (trimmed from a W36×256 section) was bolted to the beam top flange and to the

Table 1. Kaiser Bolted Bracket Proportions						
Bracket Designation	Bracket Length, L_{bb} in. (mm)	Bracket Height, h_{bb} in. (mm)	Bracket Width, b_{bb} in. (mm)	Number of Column Bolts, n_{cb}	Column Bolt Gage, g in. (mm)	Column Bolt Diameter in. (mm)
W3.0	16 (406)	5½ (140)	9 (229)	2	5½ (140)	1⅜ (35)
W3.1	16 (406)	5½ (140)	9 (229)	2	5½ (140)	1½ (38)
W2.0	16 (406)	8¾ (222)	9 (229)	4	6 (152)	1⅜ (35)
W2.1	18 (457)	8¾ (222)	9½ (241)	4	6½ (165)	1½ (38)
W1.0	25½ (648)	12 (305)	9½ (241)	6	6½ (165)	1½ (38)
B2.1	18 (457)	8¾ (222)	10 (254)	4	6½ (165)	1½ (38)
B1.0	25½ (648)	12 (305)	10 (254)	6	6½ (165)	1½ (38)
B1.0C	28¾ (730)	12 (305)	10 (254)	6	6½ (165)	1⅝ (41)

column face using A490 bolts. Both of the enhanced specimens exceeded the AISC *Seismic Provisions* (AISC, 2005a) SMF qualifying requirements.

The research concluded that with adequately proportioned brackets, a repaired connection can redirect the flange tension force, thereby reducing the stress in the flange welded joints. In addition, the global study concluded that the presence of a concrete floor slab was beneficial to specimen performance by enhancing beam stability and delaying strength degradation (Gross et al., 1999).

CAST KAISER BOLTED BRACKET DEVELOPMENT

Following the successful completion of the Lehigh bolted bracket testing, research objectives focused on utilizing a high-strength casting as a replacement for the welded plate bracket. Fabrication of the plate brackets required a significant amount of skilled labor and rigorous inspection, while a one-piece casting could be manufactured in a quality consistent process, with little or no skilled labor.

In accordance with the design provisions outlined by Gross et al. (1999), two cast bracket configurations were developed and the concept was patented with the United States Patent and Trademark Office. The first configuration or W-series bracket is shop fillet-welded to a beam flange. As shown in Figure 2, the horizontal flanges of the W-series brackets are tapered to permit the application of a connecting fillet-weld to the beam flange.

The second configuration or B-series brackets are bolted to a beam flange. As shown in Figure 3, the horizontal flange of the B-series brackets are cast with two rows of parallel bolt holes. While initially intended for the repair of damaged moment connections, the bolted B-series may also be used in new moment frame construction, where a bolted application can facilitate fabrication. Once connected, the design intent is to promote yielding and plastic hinge formation in the beam at the end of the connected brackets.

Based on recommendations from the Steel Founder's Society of America (SFSA), the bracket cast steel specification was designated A148 Grade 80/50, the predecessor to the current specification of A958 Grade SC8620 class 80/50 (ASTM, 2006). The cast steel material has a nominal yield and tensile strength of 50 ksi (354 MPa) and 80 ksi (566 MPa), respectively.

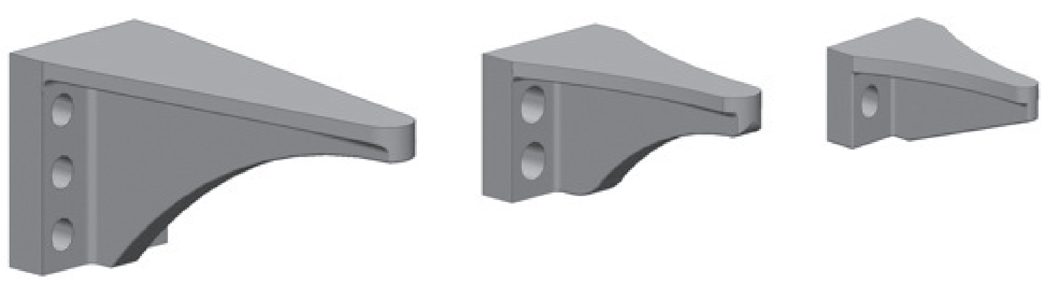

(a) Six-bolt W1.0 *(b) Four-bolt W2.1/W2.0* *(c) Two-bolt W3.1/W3.0*

Fig. 2. W-series bracket.

Table 2. W-Series Bracket Design Proportions						
Bracket Designation	**Column Bolt Edge Distance, d_e in. (mm)**	**Column Bolt Pitch, p_b in. (mm)**	**Bracket Stiffener Thickness, t_s in. (mm)**	**Bracket Stiffener Radius, r_v in. (mm)**	**Bracket Horizontal Radius, r_h in. (mm)**	**Minimum Fillet Weld Size in. (mm)**
W3.0	2½ (64)	None	1 (25)	n.a.	28 (711)	½ (13)
W3.1	2½ (64)	None	1 (25)	n.a.	28 (711)	⅝ (16)
W2.0	2¼ (57)	3½ (89)	2 (51)	12 (305)	28 (711)	¾ (19)
W2.1	2¼ (57)	3½ (89)	2 (51)	16 (406)	38 (965)	⅞ (22)
W1.0	2 (51)	3½ (89)	2 (51)	28 (711)	n.a.	⅞ (22)

Table 3. B-Series Bracket Design Proportions						
Bracket Designation	**Column Bolt Edge Distance, d_e in. (mm)**	**Column Bolt Pitch, p_b in. (mm)**	**Bracket Stiffener Thickness, t_s in. (mm)**	**Bracket Stiffener Radius, r_v in. (mm)**	**Number of Beam Bolts, n_{bb}**	**Beam Bolt Diameter in. (mm)**
B2.1	2 (51)	3½ (89)	2 (51)	16 (406)	8	1⅛ (29)
B1.0	2 (51)	3½ (89)	2 (51)	28 (711)	12	1⅛ (29)
B1.0C	2 (51)	3½ (89)	2 (51)	32 (813)	14	1¼ (32)

The A958 specification imposes a number of requirements beyond identifying the casting steel material. The specification requires the castings be produced in conjunction with a heat treatment process that includes normalizing and stress relieving and requires each batch of steel meet strict mechanical and chemical composition properties. These properties include the specified tensile and yield strengths, as well as elongation and area reduction limitations.

Following production, visual inspection and nondestructive quality control measures are performed on the castings. The nondestructive measures include tensile, radiographic, ultrasonic and magnetic particle testing.

Connection detailing for the Kaiser brackets is shown in Figure 4. The corresponding bracket proportions are summarized in Table 1. The design proportions for the W- and B-series bracket configurations are further summarized in Tables 2 and 3, respectively. In order to accommodate attachment of a fillet weld to the W-series brackets, the beam flange must be at least 6 in. (152 mm) wide. When specifying the B-series brackets, to prevent beam flange tensile rupture, the beam flange must be at least 9 in. (254 mm) wide.

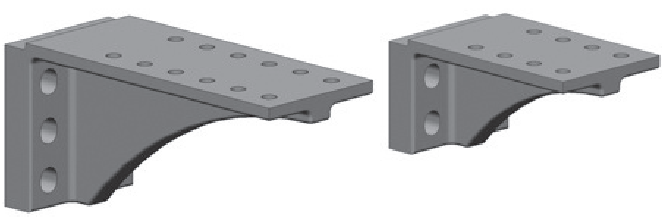

(a) Six-bolt B1.0/B1.0C *(b) Four-bolt B2.1*

Fig. 3. B-series bracket.

As shown in Figures 2(b), 2(c) and 3(a), a dual designation is associated with each of the depicted brackets. The difference between the two designations is the column bolt diameter, the bracket length, or both as indicated in Table 1.

The fasteners connecting the bracket to the beam and column are high-strength pretensioned A490, F2280 or A354 grade BD bolts. In the B-series brackets, when retrofitting an existing connection, the bracket-to-column bolt hole is cast with a standard bolt diameter and the bracket-to-beam bolts holes are cast 1⁄16 in. (2 mm) smaller than the nominal bolt diameter. Otherwise, the bracket-to-column holes are cast vertically short-slotted for field installation tolerance.

The matching bolt holes in the column and beam flanges are drilled ⅛ in. (3 mm) and 1⁄32 in. (1 mm) larger than the nominal bolt diameter, respectively. For the B-series, the bracket is typically used as a template to drill the beam flange bolt holes and simultaneously chase the holes in the casting. The strict tolerance on the beam flange bolt holes reduces the potential for connection slip.

For the W-series brackets, the filler metal used to weld the bracket to the beam flange requires rated notch toughness in accordance with Section 7.3b of the AISC *Seismic Provisions* (AISC, 2005a).

When necessary, finger shims are used to fill the gap between the column flange and the bracket. However, the use of finger shims is subject to the limitations of RCSC *Specification for Structural Joints Using ASTM A325 and A490 Bolts* (RCSC, 2004).

The beam shear tab is a single plate connected to the column flange using a two-sided fillet weld, a two-sided partial-joint-penetration (PJP) groove weld or CJP groove weld. The shear tab is fastened to the beam with A325 bolts.

The thick rear flange of the bracket is designed to eliminate prying action in the bolts. However, prying action is still a design consideration in the connecting column flange.

As shown in Figure 4, the connection of the bracket to the column increases the effective panel zone depth. The increase in depth increases the area of the panel zone and can reduce or, in some cases, eliminate the need for doubler plates in accordance with the requirements of the AISC *Seismic Provisions* (AISC, 2005a).

Continuity plates have been a feature for many code prequalified moment connections. These stiffeners, positioned horizontally on each side of the column, are welded to the flanges and to the web. The use of continuity plates is dictated by the need to satisfy code prescribed limit states for the flange and web of the column. In a bolted connection, the configuration of the fasteners can impede the ability of the stiffeners to effectively address these limit states. The design intent for the KBB connection is to satisfy the prescribed limit states without continuity plates.

CONNECTION EXPERIMENTAL EVALUATION

The effectiveness of the KBB moment-resisting connection has been demonstrated experimentally at both Wyle Laboratories (Norco, California) and at the University of California, San Diego (UCSD). At Wyle Labs, a total of six tests were performed in 1998. Three of the tests were performed to obtain approval from the California Office of Statewide Healthcare Planning and Development (OSHPD) for a hospital moment frame retrofit project and the remaining three to obtain general approval from Los Angeles County for a variety of planned new moment frame projects. At UCSD, a test was performed in July 2005 to determine if the connection was a viable alternative for a moment frame retrofit project in Oakland, California (Newell and Uang, 2006).

Test Matrix

The experimental evaluation involved the testing of seven full-scale KBB connection subassemblies. The test matrix is shown in Table 4, and the details of the specimens are summarized and discussed herein. The test specimens included a wide range of

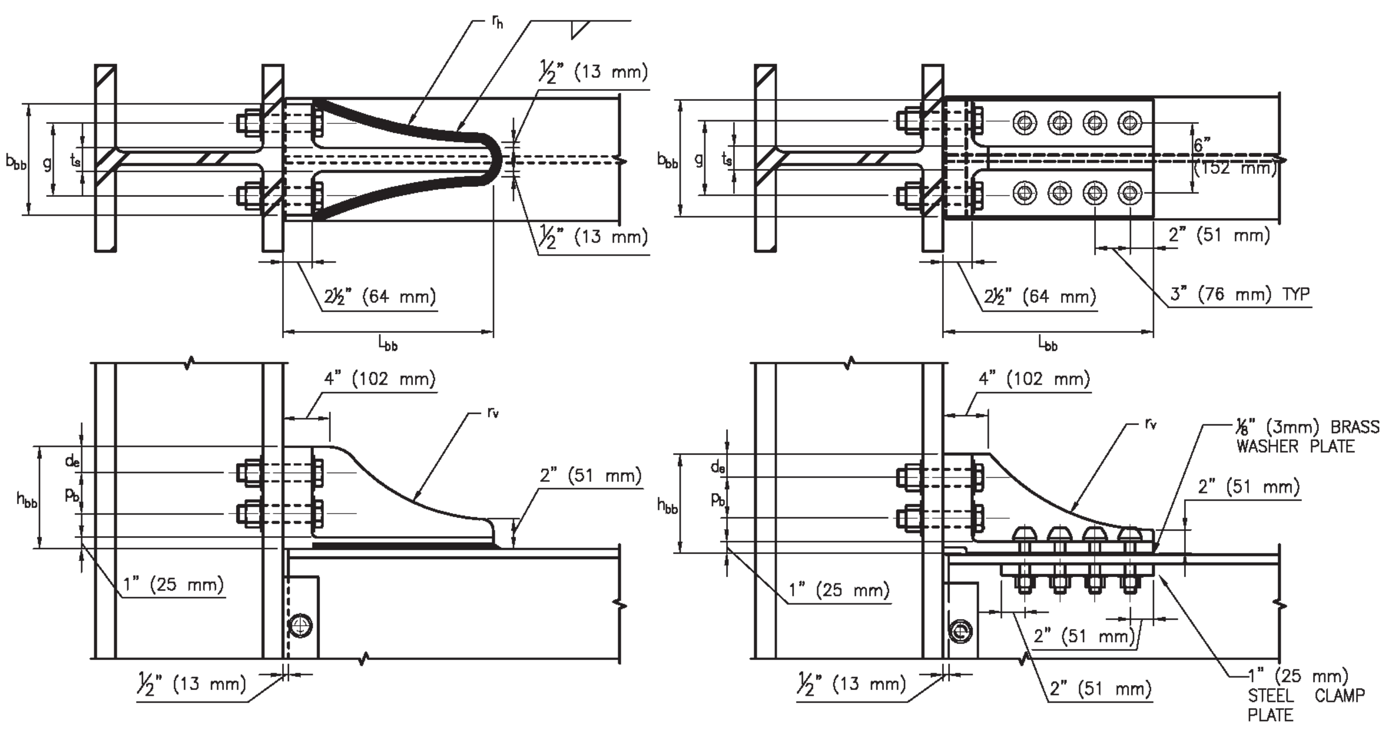

(a) W-series (b) B-series

Fig. 4. Kaiser bolted bracket connection detailing.

Table 4. Test Specimen Matrix										
Specimen Designation	Column Size	Beam Size	Bracket Size	Column Type	Floor Slab	Span-to-Depth Ratio	$\frac{\Sigma M^*_{pc}}{\Sigma M^*_{pb}}$	Panel Zone $\phi_v R_v/R_u$	Continuity Plates t_{cf}/t_{req}	Loading Sequence
HH-5	Box[a]	W33×130	B1.0	Interior	No	11	0.8	1.0	1.4	ATC-24
HH-5A	Box[a]	W33×130	B1.0	Exterior	No	11	1.3	2.1	1.4	ATC-24
HH-6	W14×233	W30×108	B2.1	Exterior	No	12	1.7	1.1	1.0	ATC-24
HH-7	W14×233	W18×55	W3.1	Exterior	No	20	5.2	2.1	1.4	ATC-24
HH-8	W14×233	W30×108	W2.1	Exterior	No	12	1.7	1.1	1.0	ATC-24
HH-9	W14×132	W24×55	W3.1	Exterior	No	15	2.3	1.1	0.9	ATC-24
UCSD-3	W27×281[b]	W36×210	B1.0C	Interior	Yes	10	0.9	0.6	0.9	AISC-341

[a] Built-up box column: 15⅝ in. (397 mm) square by 1½ in. (38 mm) thick, 288 lb/ft (432 kg/m) total weight
[b] Panel zone strengthened with a ⅜–in. (10–mm) doubler plate (one side) and ⅝–in. (16–mm) continuity plates (both sides)

conditions and applications. Two of the specimens, HH-5 and UCSD-3, represented an interior moment frame column, with one specimen, HH5A, representing a three-sided condition when attached in conjunction to the column of specimen HH-5. One of the specimens, UCSD-3, had a composite concrete floor slab. In this test, to facilitate instrumentation, the concrete slab was blocked out around the brackets. In four of the test specimens, HH5, HH-5A, HH-6 and USCD-3, the bracket was bolted to the beam. These four specimens represented existing moment frame connections under consideration for retrofitting using the bolted bracket. The remaining specimens, HH-7, HH-8 and HH-9, were fillet-welded to the beam to represent new moment frame connections under consideration for construction.

The specimen column sizes ranged from a W14×132 to a W27×281 and included a square box column. The specimen beam sizes ranged from a W18×55 to a W36×210. All of the specimens had nominal steel yield strengths of 50 ksi (345 MPa). The cast Kaiser bracket sizes ranged from a W3.1 to a B1.0C. Each basic bracket size was represented. The clear span-to-depth ratio of the specimens varied between 10 and 20.

Included in Table 4 are the column-beam moment ratios prescribed by the AISC *Seismic Provisions* (AISC, 2005a). The criteria require the columns to be generally strong enough to force flexural yielding in the beam, thereby avoiding the formation of single-story mechanism. Two of the specimens, HH-5 and UCSD-3, both representing existing conditions, did not satisfy the criteria. The criteria are satisfied when the ratio of the sum of the column nominal flexural capacity, ΣM^*_{pc}, to the sum of the beam expect flexural capacity, ΣM^*_{pb}, is greater than 1.0 for each specimen, where the flexural capacities are extrapolated to the intersection of the beam and column centerline in accordance with the AISC *Seismic Provisions* (AISC 2005a).

Also included in Table 4 are the column panel zone (PZ) ratios prescribed by the AISC *Seismic Provisions* (AISC, 2005a). The criteria require minimum strength to prevent excessive column PZ distortion, where the strength, R_v, and the demand, R_u, are defined in accordance with the AISC *Seismic Provisions* (AISC, 2005a).

For reference purposes, Table 4 also includes the continuity plate criteria outlined in AISC *Prequalified Connections for Special and Intermediate Steel Moment Frames for Seismic Applications* (AISC, 2005c), hereafter referred to as the AISC *Prequalified Connections*. The criteria require minimum column flange thickness, t_{cf}, to prevent local flange buckling and to help distribute beam flange forces to the column web.

In order to evaluate the performance of the connection without continuity plates, the wide flange column specimens at Wyle Labs were tested without the stiffeners, with the condition for specimen HH-9 being unconservative. In specimen UCSD-3, continuity plates were provided at the same level as the beam flange.

Material Properties

The beams and columns for specimens HH-5 through HH-9 were fabricated from A572 Grade 50 steel. The beams and column for UCSD specimen were fabricated from A992 steel. The Kaiser bolted brackets were fabricated from A148 Grade 80/50 or 90/60 steel. Table 5 shows the measured static yield and tensile strengths, elongations, heat numbers and material suppliers for the test members. The mechanical properties were determined from tensile coupon tests and certified mill test reports. The cast steel tensile coupons or keel blocks were taken from the same heat as the representative casting in accordance with ASTM standards (ASTM, 2006). Fillet welds connecting the W-series bracket to the

Table 5. Steel Mechanical Properties

Member	Size	Steel Grade	Location	Yield Strength[a] ksi (MPa)	Tensile Strength[a] ksi (MPa)	Elongation[a] (%)	Heat Number	Supplier
Column	Box	A572 Gr. 50	Flange	58.2 (402)	85.9 (592)	[18]	2C7673	Geneva
Column	W14×233	A572 Gr. 50	Flange	46.5 (321)	65.7 (453)	[24]	70731	Kawasaki
Column	W14×132	A572 Gr. 50	Not taken	[57.0 (393)]	[76.0 (524)]	[28]	1-44900	Kawasaki
Column	W27×281	A992	Flange	54.4 (375)	74.6 (515)	33	234974	Nucor-Yamato
Column	W27×281	A992	Web	57.2 (395)	75.1 (518)	34	234974	Nucor-Yamato
Beam	W33×130	A572 Gr. 50	Flange	53.6 (370)	73.0 (504)	[22]	83254	Nucor-Yamato
Beam	W30×108	A572 Gr. 50	Flange	55.7 (384)	75.0 (518)	[25]	2-40010	Kawasaki
Beam	W30×108	A572 Gr. 50	Flange	53.0 (366)	67.0 (462)	[25]	2-40010	Kawasaki
Beam	W24×55	A572 Gr. 50	Flange	51.0 (352)	71.0 (490)	[26]	102958	Nucor-Yamato
Beam	W18×55	A572 Gr. 50	Not taken	[56.0 (386)]	[70.0 (483)]	[29]	3-5006	Chaparral
Beam	W36×210	A992	Flange	52.0 (359)	73.0 (504)	34	226190	Nucor-Yamato
Beam	W36×210	A992	Web	67.6 (466)	77.0 (531)	26	226190	Nucor-Yamato
Bracket	B1.0	A148 Gr. 80/50	Keel block	60.0 (414)	87.0 (600)	25	8/21/97-H3	Varicast
Bracket	W3.1	A148 Gr. 80/50	Keel block	61.0 (421)	88.0 (607)	22	12/31/97-H7	Varicast
Bracket	B2.1	A148 Gr. 80/50	Keel block	61.3 (423)	87.9 (607)	24	12/06/97-H3	Varicast
Bracket	W2.1	A148 Gr. 80/50	Keel block	73.9 (510)	102.9 (710)	22	H-3781	Pacific Steel
Bracket	B1.0C	A148 Gr. 90/60	Keel block	73.8 (365)	96.4 (90.0)	22	6336	North Star

[a] Values in brackets are based on Certified Mill Test Reports, others from coupon testing

beam were made from rated notch toughness E71-T8 filler metal. Further details regarding material properties for the UCSD specimen are reported in Newell and Uang (2006).

Test Subassemblage, Loading Protocol and Instrumentation

The subassemblage for the tests performed at Wyle Labs positioned the specimens in a horizontal plane just above the test floor as shown in Figure 5. The ends of the columns had pin-connected boundary conditions, using cylindrical bearings to simulate inflection points at the column mid-height in the prototype frame. The actuator attachment was made near the end of each beam through a load transfer assembly and lateral supports were provided along the beams as shown. The Kaiser brackets were attached to the beam and column specimens as indicated in Figure 4. The W-series brackets were fillet welded to the beam using a weld procedure specification (WPS) qualified for the combination of cast and rolled materials.

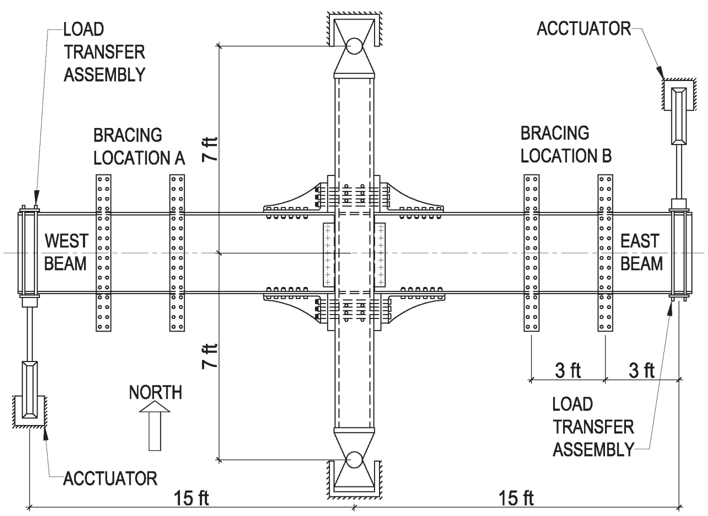

Fig. 5. Wyle Labs horizontally positioned experimental test setup. (Note: 1 ft = 305 mm)

Table 6. Summary of Test Results					
Specimen Designation	Maximum Interstory Drift Angle (% rad)	Maximum Inelastic Drift Angle (% rad)	Maximum Column Face Moment Ratio, M_{cf}/M_p	Maximum Plastic Hinge Moment Ratio, M_{ph}/M_p	Test Failure Mode
HH-5	6.1	4.7	1.51	1.25	No failure, maximized actuator stroke
HH-5A	6.8	5.1	1.55	1.29	No failure, maximized actuator stroke
HH-6	4.6	3.0	1.22	1.09	No failure, slip in the test apparatus
HH-7	4.8	3.1	1.37	1.24	Flange gross area fracture
HH-8	5.6	4.6	1.31	1.18	No failure, excessive buckling in specimen
HH-9	6.9	6.0	1.38	1.25	No failure, maximized actuator stroke
UCSD-3	4.0	3.0	1.35	1.11	Bracket-to-column bolt tensile rupture

The subassemblage for the test performed at UCSD positioned the specimen in a vertical plane. Pins were provided at the ends of the beams and at the top and bottom of the column to simulate inflection points. The actuator attachment was made at the top of the column through a load transfer assembly. Further details regarding the subassemblage including lateral bracing, steel column guides, composite floor connections and other details is reported by Newell and Uang (2006).

The specimens were tested by imposing a prescribed quasi-static cyclic story drift history. At UCSD, the loading history was based on the protocol specified in Appendix S of the AISC *Seismic Provisions* (AISC, 2005a). In this sequence deformations consist of six cycles each of 0.375, 0.5 and 0.75% story drift, followed by four cycles of 1.0% story drift and two cycles each of 1.5, 2, 3, 4 and 5% story drift.

At Wyle Labs, the loading history was based on the protocol specified in ATC 24 (ATC, 1992), which is considered acceptable by the AISC *Seismic Provisions* (AISC, 2005a). In this sequence, deformations are applied to the test specimen, up to the completion of the test, to produce three cycles each of loading at $0.25\delta_y$, $0.68\delta_y$, δ_y, $2\delta_y$, $3\delta_y$, followed by two cycles each of loading at $4\delta_y$, $5\delta_y$, $6\delta_y$, where δ_y is the deformation value at the first significant yield of the test specimen.

The testing was terminated when a fracture occurred, resulting in a significant loss of beam capacity; when the testing apparatus became unstable; or after reaching the equivalent story drift of $6\delta_y$, where $6\delta_y$ was the maximum stroke the actuator could accommodate.

As reported by Newell and Uang (2006), the test specimen at UCSD was instrumented to enable measurement of the applied loads, strains in the beams, column, brackets and panel zone, in addition to panel zone and bracket deformation. The beams, column and panel zone in the connected region were whitewashed prior to testing to provide visual indication of the occurrence of yielding during testing. The test specimens at Wyle Labs were instrumented to enable measurement of the applied loads, strains in the beams, column, brackets and panel zone. The panel zone deformation was not instrumented.

Test Results

All the specimens tested at Wyle Labs exceeded the AISC *Seismic Provisions* (AISC, 2005a) SMF qualifying 4.0% interstory drift angle without significant strength degradation. The UCSD test specimen met the requirement but subsequently experienced an unexpected nonductile connection failure. A summary of the response for each specimen is shown in Table 6, including the maximum interstory drift angle, the corresponding maximum inelastic drift angle, maximum column face moment ratio, maximum plastic hinge moment ratio and the test failure mode.

The interstory drift angle was computed by taking the beam tip displacement and dividing by the distance to the column centerline. The inelastic drift angle was calculated by taking the inelastic portion of the tip deflection and dividing by the distance to the face of the column. The beam column face moment, M_{cf}, was computed by taking the maximum force applied at the beam tip multiplied by the distance to the column face. The beam plastic hinge moment, M_{ph}, was computed by taking the maximum force applied at the beam tip multiplied by the distance to the end of the bracket. The column face and plastic hinge moment ratios are calculated by dividing the respective moment by the corresponding beam nominal plastic moment, M_p.

Figure 6 (pp. 190–191) shows plots of the applied load versus beam tip displacement for each specimen tested at Wyle Labs. The corresponding beam moment and interstory drift angle are also shown on the plots. The 4.0% interstory drift angle is shown with vertical dashed lines and the 80%

nominal plastic moment is shown with horizontal dashed lines corresponding to the AISC *Seismic Provisions* (AISC, 2005a) strength degradation requirement. As indicated in Figure 6, each of the specimens underwent a gradual deterioration of strength following the onset of local flange and web buckling of the beam. This gradual reduction in strength typically occurred after about 3.0 to 4.0% drift.

Specimens HH-5 and HH-5a were erected and tested separately on the opposing faces of the same built-up box column. As mentioned previously, the test was intended to represent an interior three-sided moment connection. A 1¾-in. (44-mm) spacer plate was positioned between the HH-5A beam flange and the brackets to offset the bolt holes projecting through the column. The hysteretic plots are shown in Figures 6(a), 6(b) and 6(c) for specimen HH-5 east beam, HH-5 west beam and HH-5A orthogonal beam, respectively. The slight pinching observed in the plots can be attributed to the slip-bearing behavior of the bolted beam flange connection. Following some amount of initial slip, subsequent hardening due to bolt bearing is observed. In specimen HH-5, panel zone yielding was observed in the column. Strain gauges were observed to be in the yield range at an interstory drift angle of approximately 3.3% drift. The same level of panel zone strain was not observed in the single-sided specimen HH-5A.

The tests were halted at 6.1% and 6.8% drift for specimen HH-5 and HH-5A, respectively, after the maximum actuator stroke was reached. At this level of rotation, a distinct plastic hinge had formed near the far end of the brackets as shown in Figures 7(a) and (b) (p. 192) for specimen HH-5 and HH-5A, respectively. Figure 7(c) shows a close-up of the beam flange near the end of the bracket in specimen HH-5 east, highlighting the ability of the thin brass washer and clamp plates to mitigate net area fracture. This detailing prevents flange buckling and abrading from distorting the first row of bolts as exhibited in earlier bolted bracket testing (Kasai et al., 1998).

Specimens HH-6 and HH-8 both used the same size beam and column. For specimen HH-6, the B-series brackets were bolted to the beam flange, and for specimen HH-8, the W-series brackets were welded to the beam flange. The test for specimen HH-6 was halted at approximately 4.6% drift to prevent damage to the test apparatus due to beam flange local buckling and column base anchorage bolt slip.

As shown in Figure 8(a) (p. 192), a 2-in. (50-mm) crack in the bracket-to beam fillet weld of specimen HH-8 was observed near the nose of the bracket at approximately 3.3% drift. Following a short pause, the test was continued with no observance of further crack growth. At approximately 5.6% drift, the test was halted to prevent damage to the apparatus due to excessive beam buckling. In both specimens HH-6 and HH-8, a plastic hinge was formed in the beam near the far end of the brackets. Figure 8(b) shows the hinge in specimen HH-8 at the end of the test.

Specimens HH-7 and HH-9 both had W-series brackets welded to the beam. The hysteretic plots are shown in Figures 6(e) and 6(g) for specimen HH-7 and HH-9, respectively. As shown in Figure 6(e), the combined strong column-weak beam and high PZ ratios focused the majority of the inelastic rotation into the beam. The test for specimen HH-7 was terminated at approximately 5.9% drift following gross area fracture in the beam flange. As shown in Figure 8(c), the fracture occurred approximately 3 in. (76 mm) from the end of the bracket in the same general vicinity where local inelastic buckling and low cyclic fatigue had weakened the lange.

The test for specimen HH-9 was halted at approximately 6.9% drift after the maximum actuator stroke was reached. At this level of rotation, a plastic hinge had formed in the beam near the far end of the brackets. Figure 9 (p. 193) shows the hinge in specimen HH-9 at the end of the test.

Specimen UCSD-3 represented an existing interior connection with a composite slab. During the test, as reported by Newell and Uang (2006), yielding in the column panel zone and in both the beam and column flanges was initially observed at approximately 0.75% drift. The column doubler plate had noticeably buckled at approximately 3.0% drift. On the first positive excursion to 4.0% drift, one of the lower bracket-to-column bolts ruptured. Despite the rupture and after a brief pause, the test was continued. On the first negative excursion to 4.0% drift, a bracket-to-column bolt on the opposite lower beam subsequently ruptured. Upon completion of the second full cycle of 4.0% drift, all the remaining lower bracket-to-column bolts ruptured, and the attaching bottom flange CJP weld fractured. Following the test, the remaining upper bolts were removed and observed to have been bent where the threaded portion of the bolt was in contact with the column flange.

Evaluation of Test Results

As indicated in Table 6, the specimen maximum plastic hinge moment ratios were similar to or less than the factor of 1.27 prescribed by AISC *Prequalified Connections* (AISC, 2005c) to account for both material overstrength, R_y, and strain hardening, C_{pr}.

Following a significant amount of inelastic strain, specimen HH-7 failed by gross area ductile fracture of the beam flange near the end of the bracket. While the cyclic loading of the remaining specimens at Wyle Labs was halted prior to fracture, given the observed cyclic inelastic strains, had the testing continued, flange gross area fracture would have been expected in these specimens as well.

As mentioned previously, the test specimens were instrumented with strain gauges to enable measurement of inelastic behavior in each of the connection components, including the beam and column flanges, the panel zone and the brackets. The component normalized tensile strains at 4.0%

Table 7. Component Normalized Tensile Strains at 4% Interstory Drift

Specimen Designation	Beam Flange Net Area	Beam Flange Gross Area	Column Flange Net Area	Column Flange Gross Area	Panel Zone	Bracket Stiffener Edge	Bracket Heel	$\frac{\Sigma M^*_{pc}}{\Sigma M^*_{pb}}$	Panel Zone $\phi_v R_v / Ru$
HH-5	6.5	3.5	1.5	1.2	0.4	4.2	0.9	0.8	1.0
HH-5A	6.5	3.5	0.5	0.7	0.2	3.3	1.0	1.3	2.1
HH-6	5.0	3.6	0.5	No Gauge	0.2	0.6	0.5	1.7	1.1
HH-7	Not bolted	7.0	0.2	0.2	0.1	0.5	0.4	5.2	2.1
HH-8	Not bolted	5.0	No Gauge	0.2	0.3	1.2	0.3	1.7	1.1
HH-9	Not bolted	4.0	0.4	0.4	0.8	0.5	0.3	2.3	1.1
UCSD-3	20.0	6.0	20	4.0	15.0	1.0	0.3	0.9	0.6

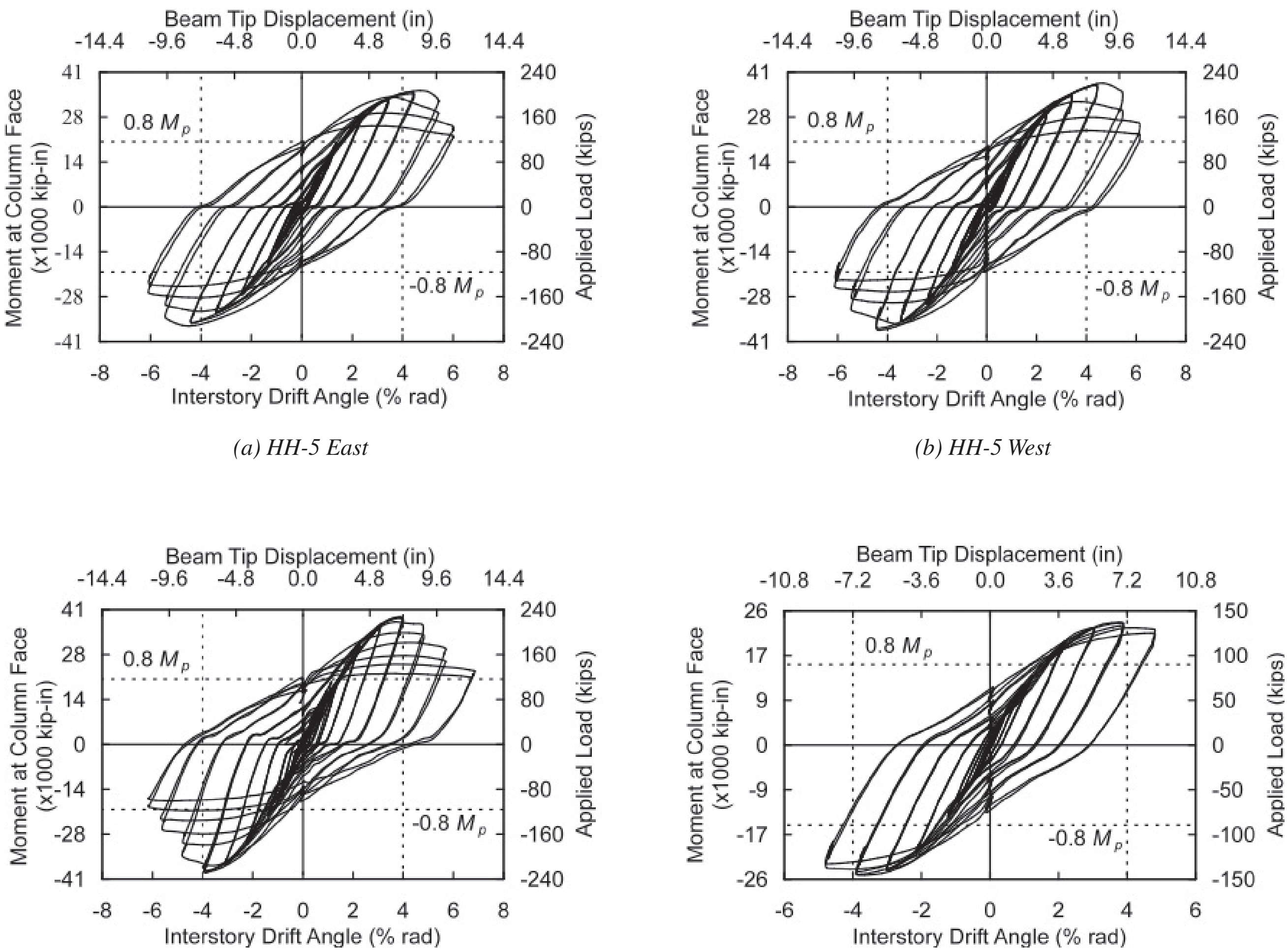

(a) HH-5 East

(b) HH-5 West

(c) HH-5A

(d) HH-6

Fig. 6. Applied load versus beam tip displacement—Wyle Labs specimens. (Note: 1 kip = 4.44 kN; 1 in. = 25.4 mm)

interstory drift are show in Table 7. In this table, the calculated column-beam and PZ ratios are repeated from Table 4 to compare with the measured strains. Although not totally inclusive of all inelastic contributions, these values indicate how each primary component contributed to the total inelastic behavior of the connection. For example, the calculations and strain measurements for specimen HH-7 indicate that virtually all the plastic rotation was developed within the beam; essentially no inelastic behavior was observed or recorded in the column, panel zone or brackets.

Each of the cast bracket stiffeners were instrumented on the free edge and near the junction of the vertical and horizontal flange (heel). As shown in Table 7, inelastic tensile strain in the brackets was limited to locations on the free edge. Following the completion of each test, no visible signs of distress to the stiffeners or to any other portion of the brackets were detected.

As described previously, and as shown in Figure 8(a), the bracket fillet weld in specimen HH-8 developed a 2-in. (50-mm) crack at the nose of the bracket. Despite the incident, the test was continued with no further observed crack growth. It is believed that the high toughness weld metal was a key factor that prevented the growth of the crack. Following the test, the procedure used to fillet weld the bracket to the beam was modified to avoid terminating weld passes near the bracket nose. Apparently, the specimen HH-8 weld passes had been terminated in this region. During the subsequent tests for specimens HH-7 and HH-9, no cracks were observed in the fillet welds made with the revised procedure.

Both column and beam flange bolt slip was observed in the test specimens. Figures 6(a) through 6(d) of the hysteretic plots show varying levels of pinching due to beam bolt slip. Column bolt slip is also evident in the hysteretic plots,

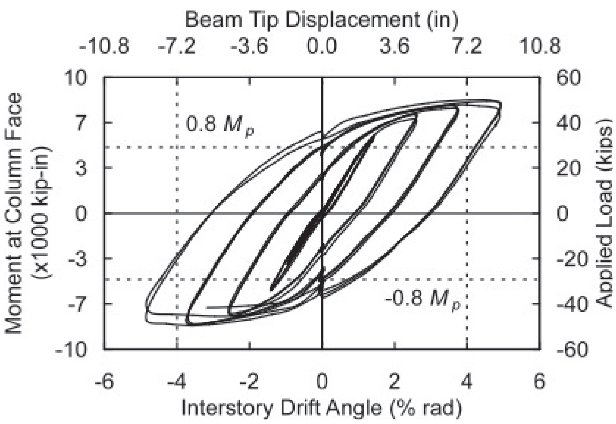

(e) HH-7

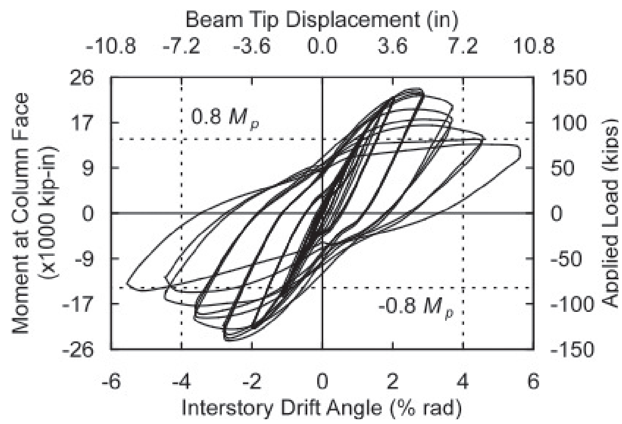

(f) HH-8

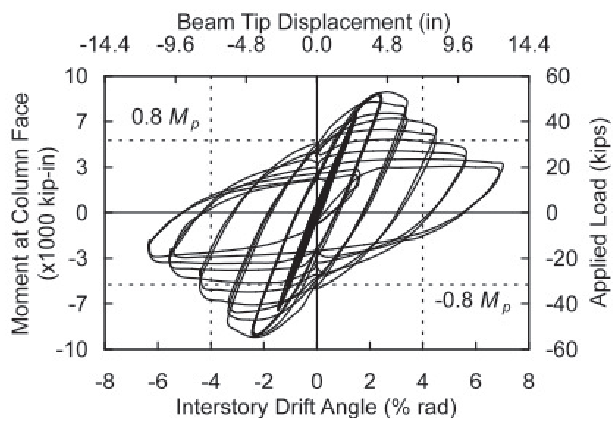

(g) HH-9

Fig. 6. (cont.) Applied load versus beam tip displacement—Wyle Labs specimens. (Note: 1 kip = 4.44 kN; 1 in. = 25.4 mm)

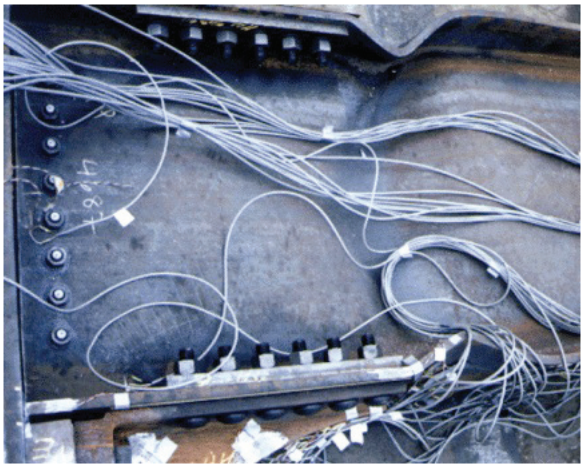

(a)

(b)

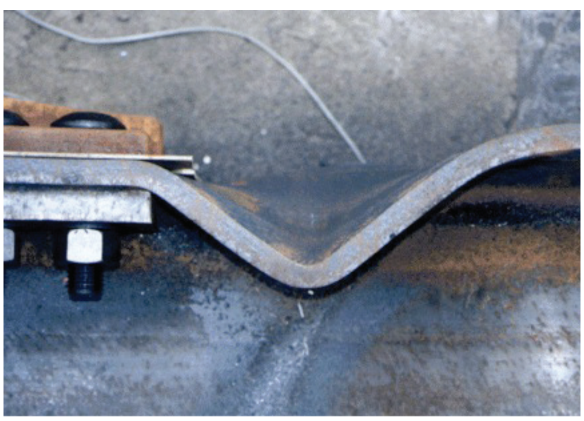

(c)

Fig. 7. Photographs of specimens at the end of testing: (a) HH-5 east beam hinge formation; (b) HH-5A hinge formation; (c) HH-5 east beam flange local buckling.

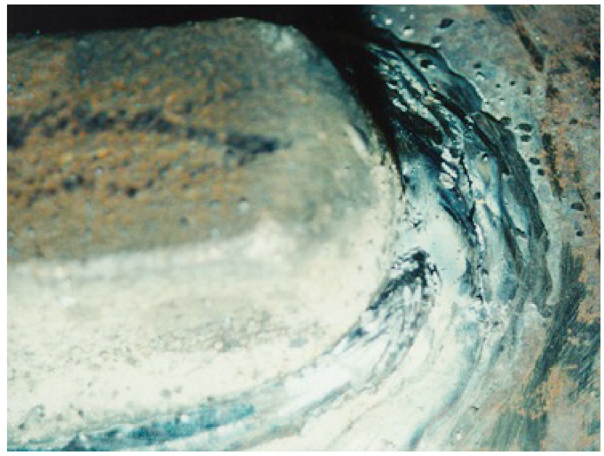

(a)

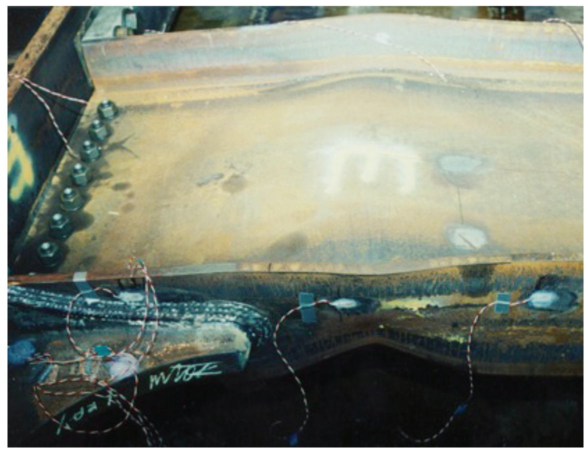

(b)

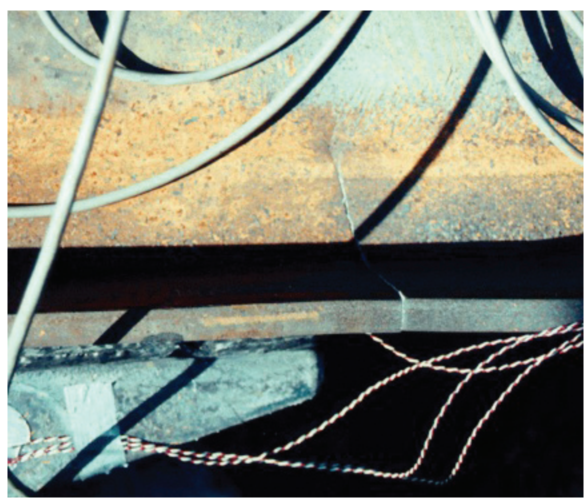

(c)

Fig. 8. Photographs of specimens at the end of testing: (a) HH-8 fillet weld crack close up; (b) HH-8 hinge formation; (c) HH-7 flange gross area fracture.

although less pronounced. In bolted connections, some amount of limited and controlled slip can be a desirable phenomenon. As a result of slippage, the stiffness of the structure decreases, the period elongates, and the energy dissipation and damping increase, all positive benefits. However, excessive slip can result in larger than expected story drifts. To limit and control slip, the B-series bracket specifies the use of smaller-diameter drilled beam bolt holes. Because the brackets can be either fastened to the beam in a fabrication shop or drilled in-place using the bracket as a template, the controlled conditions permit the strict tolerance required by the smaller-diameter hole.

In the Wyle Labs wide flange columns specimens, the tests were intended to evaluate the performance of the connection without continuity plates. In those specimens, the absence of continuity plates did not appear to promote local flange buckling or lead to other detrimental effects.

In specimen UCSD-3, significant yielding was observed and recorded in the panel zone. Analysis of the test data for specimen UCSD-3 indicated that between one-half and two-thirds of the total plastic rotation was developed by panel zone yielding, with the remainder developed by yielding in the beams and columns, particularly in the flange net areas (Newell and Uang, 2006). As shown in Table 7, measured inelastic strain in the panel zone was significant. Given the

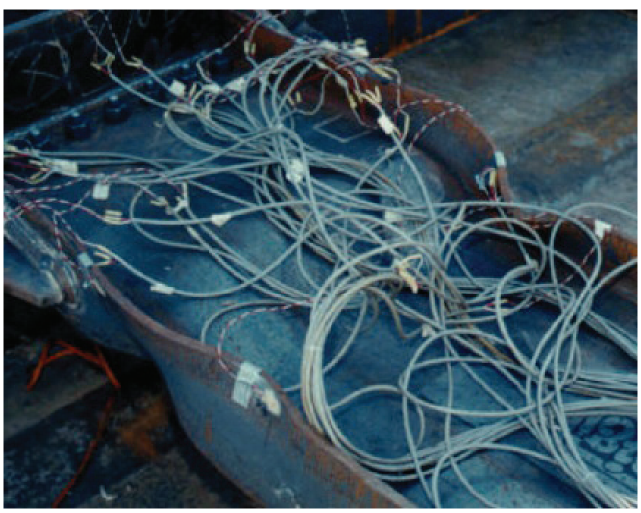

Fig. 9. Photograph of hinge formation at the end of testing specimen HH-9.

panel zone yielding and the observed bending in the remaining bracket-to-column bolts, deformation of the connecting column likely caused bolt tensile force levels to increase above their ultimate strength and fail. As indicated by the AISC *Steel Construction Manual* (AISC, 2005d), hereafter referred to as the AISC *Manual*, this prying action phenomenon can significantly increase the tensile force in a bolt.

Subsequent analysis of specimen UCSD-3 also determined several unintentional column limit state deficiencies. As indicated in Table 7, the column strength was significantly lower than that of the attaching beams. This condition can promote the formation of a hinge in the column, typically just below the level of the stiffened region. Table 4 indicates the column was also susceptible to local flange buckling. Although equipped with a continuity plate, the position of the bracket below the stiffener does not adequately limit flange buckling due to the offset distance. Finally, analysis of the column indicated the flange bolt holes did not satisfy the tensile rupture limit state provisions of AISC 360 *Specification for Structural Steel Buildings* (AISC, 2005b). Had the column satisfied these critical limit state design provisions, a more desirable ductile failure mode would have been anticipated. Although the specimen satisfied the SMF requirements for drift and strength, as part of this evaluation, the results are not considered justification to prequalify the specimen column, beam and bracket combination.

The presence of a composite floor slab on specimen UCSD-3 did not appear to promote the bolt fracture or lead to other detrimental effects. On the contrary, the presence of the slab was beneficial to specimen performance by enhancing beam stability and delaying strength degradation despite the high levels of recorded inelastic strain.

Although specimen UCSD-3 incorporated the use of a deep column section, the majority of bolted bracket specimens have been tested with W14 columns. In previous testing of RBS connections with deeper column sections, Ricles et al. (2004) concluded that the deeper columns do not behave substantially different from W14 columns and that no special consideration or bracing was needed when a slab is present.

The limited number of tests conducted in this program is insufficient to prequalify beams larger than those tested at Wyle Labs. However, the results can be used to develop design provisions for equivalent sized beam and bracket combinations. Those provisions, currently under development, will be the focus of a future paper.

SUMMARY AND CONCLUSIONS

An experimental study was performed to investigate the Kaiser bolted bracket steel moment-resisting connection. The study included a review of historical bolted bracket tests and the evaluation of seven full-scale specimens using a high-strength cast steel bracket. The parameters investigated in the experimental program included (1) column size, (2) beam size, (3) bracket size, (4) bracket connections, (5) and clear span-to-depth ratios. The conclusions that follow are based on the test results of this study.

1. For new construction, the KBB connection is able to satisfy the criteria in Appendix S of the AISC *Seismic Provisions* (AISC, 2005a) for qualifying a connection for use in a special moment frame. The connection directs yielding and inelastic beam deformation away from the column face and outside the connected region.

2. For existing connections, the KKB connection is capable of improving the capacity of weakened or damaged moment connections. A bottom-only bracket configuration is not recommended when used in conjunction with low notch toughness (pre-Northridge) CJP weld connecting the top flange.

3. For the range of column sizes investigated in this study, it is recommended that deep and box columns be considered for prequalification. Based on the similarity in performance to that of the RBS connection, the expected column sizes would include an equivalent depth up to a W36 section. The use of box columns participating in orthogonal moment frames is also recommended. There was insufficient testing to determine if box column depths deeper than 16 in. (406 mm) should be considered.

4. For the range of W14 column sections investigated in this study, the lack of continuity plates did not have a significant effect on performance. It is recommended that the stiffeners be eliminated when the column flange thickness satisfies local flange buckling limit state requirements. There was insufficient testing to determine if deeper column sections can tolerate the removal of continuity plates. Therefore, in deeper sections, continuity plates are recommended at the same elevation as that of the beam flanges.

5. For the range of beam and bracket sizes investigated in this study, it is recommended that beam sizes be limited to an equivalent beam depth of a W33 section and a maximum beam weight of 130 lb/ft (195 kg/m) with a clear span-to-depth ratio of 8 or greater.

6. For bolted connections, deformation of the connecting column flange can increase the tensile force in the bolt above that due to the direct tensile force alone. It is recommended that the prying action specification requirements of the AISC *Manual* (AISC, 2005d) be considered when calculating the size of the fastener.

7. To avoid the formation of discontinuities in the fillet welds connecting the W-series bracket to the beam flange, it is recommended that weld passes should not be stopped or started within 2 in. (51 mm) of the bracket nose and should be continuous around the nose. In addition, the use of a high toughness weld metal is recommended.

8. In the B-series brackets, beam net area fracture, common in bolted flange connections, can be mitigated with special detailing including the use of a thin brass washer plate at the bracket-to-beam interface and clamp plates opposite the connected bracket.

9. Connection slip in beams with bolted flange connections can be controlled and limited with a strict tolerance on the drilled bolt hole diameter.

ACKNOWLEDGMENTS

The research in this paper was partially provided with the financial support of Steel Cast Connections (www.steelcast-connections.com) of Seattle, Washington, which is the current patent holder of the Kaiser bolted bracket. The authors wish to thank Mr. Ian C. Hodgson of Lehigh University for providing information on the initial bracket testing performed at Lehigh University; Mr. David Bleiman of Rutherford & Chekene, whose work at IFC Kaiser Engineering led to the development of the Kaiser brackets and who supervised the testing performed at Wyle Labs; Dr. Chia-Ming Uang and Mr. James Newell of the University of California, San Diego, who supervised the testing performed at UCSD; and Mr. Ronald Hamburger of Simpson Gumpertz & Heger, who provided a technical review of this manuscript.

The writers are solely responsible for the accuracy of statements or interpretation contained in this publication. No warranty is offered with regard to the results, findings and recommendations contained herein by Steel Cast Connections, LLC. The organization and authors do not assume any legal liability or responsibility for the accuracy, completeness or usefulness of any of the information, product or processes included in this publication.

REFERENCES

AISC (2005a), *Seismic Provisions for Structural Steel Buildings,* AISC/ANSI 341-05, American Institute of Steel Construction Inc., Chicago.

AISC (2005b), *Specification for Structural Steel Buildings,* AISC/ANSI 360-05, American Institute of Steel Construction Inc., Chicago.

AISC (2005c), *Prequalified Connections for Special and Intermediate Steel Moment Frames for Seismic Applications,* AISC/ANSI 358-05, American Institute of Steel Construction, Chicago.

AISC (2005d), *Steel Construction Manual,* 13th ed., American Institute of Steel Construction, Chicago.

ATC (1992), *Guidelines for Cyclic Seismic Testing of Components of Steel Structures,* ATC-24, Applied Technology Council, Redwood City, CA.

ASTM (2006), "Standard Specification for Steel Castings, Carbon and Alloy, with Tensile Requirements, Chemical Requirements Similar to Standard Wrought Grades," ASTM Standard A958-00 (Reapproved 2006), American Society for Testing and Materials, West Conshohocken, PA.

Anderson, J.C. and Linderman, R.R. (1991), "Post Earthquake Repair of Welded Moment Connections," *Report No. CE 91-04*, Department of Civil Engineering, University of Southern California, Los Angeles.

Engelhardt, M.D. and Sabol, T.A. (1994), "Testing of Welded Steel Moment Connections in Response to the Northridge Earthquake," *Northridge Steel Update*, American Institute of Steel Construction, Chicago.

FEMA (2000), *Recommended Seismic Design Criteria for New Moment-Resisting Steel Frame Structures,* Report No. FEMA 350, Federal Emergency Management Agency, Washington, DC.

Grigorian, C.E., Yang, T.S. and Popov, E.P. (1992), "Slotted Bolted Connection Energy Dissipators," *EERC Report No. 92/10*, Earthquake Engineering Research Center, University of California, Berkeley, CA.

Gross, J.L., Engelhardt, M.D., Uang C.M., Kasai, K. and Iwankiw, N.R. (1999), "Modification of Existing Welded Steel Moment Frame Connections for Seismic Resistance," *AISC Design Guide No. 12*, American Institute of Steel Construction, Chicago.

Kasai, K., Hodgon, I. and Bleiman, D. (1998), "Rigid-Bolted Repair Methods for Damaged Moment Connections," *Engineering Structures,* Vol. 20, No. 4–6, pp. 521–532.

Newell, J. and Uang, C.M. (2006), "Cyclic Testing of Steel Moment Connections for the CALTRANS District 4 Office Building Seismic Rehabilitation," *UCSD Report No. SSRP-05/03*, University of California, San Diego.

RCSC (2005), *Specification for Structural Joints Using ASTM A325 or A490 Bolts,* Research Council on Structural Connections, Chicago.

Ricles, J.M., Zhang, X., Lu L.W. and Fisher, J. (2004), "Development of Seismic Guidelines for Deep-Column Steel Moment Connections," *ATLSS Report No. 04-13*, Lehigh University, Bethlehem, PA.

Tremblay, R., Timlez, P., Bruneau, M. and Filiatrault, A. (1995), "Performance of Steel Structures During the 1994 Northridge Earthquake," *Canadian Journal of Civil Engineering,* Vol. 22.

Youssef, N.F.G., Bonowitz, D. and Gross, J.H. (1995), "A Survey of Steel Moment-Resisting Frame Buildings Affected by the 1994 Northridge Earthquake," *Report No. NISTIR 5625*, National Institute of Standards and Technology, Gaithersburg, MD.